

ULTIMATE BEHAVIOUR OF CONTINUOUS COMPOSITE CONCRETE SLABS

Alireza GHOLAMHOSEINI

*Post-doctoral Fellow, The University of Canterbury, Christchurch, NZ
alireza.gholamhoseini@canterbury.ac.nz*

Ian GILBERT

*Professor, The University of New South Wales, Sydney, Australia
i.gilbert@unsw.edu.au*

Mark BRADFORD

*Professor, The University of New South Wales, Sydney, Australia
m.bradford@unsw.edu.au*

Keywords: Continuous Composite Slab, Cracking, Longitudinal Shear, Steel Decking, Ultimate Strength

ABSTRACT

Composite one-way concrete slabs with profiled steel decking as permanent formwork are commonly used in the building construction industry. In addition to carry the gravity loads, composite slabs act as a diaphragm to distribute the lateral (wind and earthquake) forces to the vertical elements of the lateral load resisting systems. As ground motions occur in both horizontal and vertical directions concurrently, many design codes consider the vertical effects of earthquake by means of introducing a static load equivalent to about 25% of the dead load applied in the upward and downward directions. Thus, the design of a composite slab as a diaphragm to carry the vertical earthquake load will be very similar to that in gravity loads.

Design codes require the experimental evaluation of the load bearing capacity of each type of steel decking using full scale tests in simple-span slabs. There is no procedure in current codes to evaluate the ultimate strength of continuous composite slabs and this is often assessed by full scale tests. This paper presents the results of three full-scale tests on continuous composite concrete slabs cast with using trapezoidal steel decking profile (KF70) that is widely used in Australia. Slab specimens were tested in four-point bending at each span with shear spans of span/4. The longitudinal shear failure of each slab is evaluated and the measured mid-span deflection, the end slip and the mid-span steel and concrete strains are also presented and discussed. The slabs are also modelled in a finite element (FE) software package using interface elements to model the contact between the steel decking and concrete slab.

INTRODUCTION

Composite slabs consisting of profiled steel decking and structural concrete are increasingly used in buildings worldwide. In this system, the steel decking is normally continuous over two-spans between the supporting steel beams and during construction the concrete is poured to form a continuous one-way composite slab. The composite action between the steel decking and the hardened concrete is dependent on the transmission of horizontal shear stresses acting on the interface between the concrete slab and the steel decking.

In addition to carry the gravity loads, composite slabs act as a diaphragm to distribute the lateral (wind and earthquake) forces to the vertical elements of the lateral load resisting systems (such as frames and structural walls). Ground motions however occur in both horizontal and vertical directions concurrently. In Northridge Earthquake (1994), a number of recorded ground accelerations indicated that the vertical component was much greater than what was typically considered in design and the effects of vertical accelerations could no longer be ignored. Hence in reality, the slab transmits the gravity load and vertical and

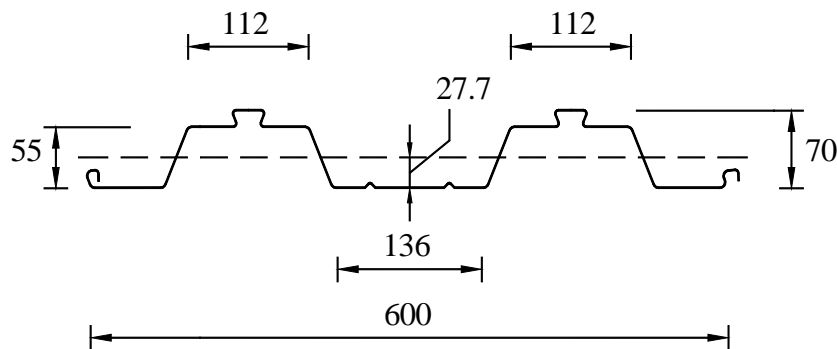
lateral component of earthquake. In many design codes the vertical effects of earthquake is considered by means of introducing a static load equivalent to about 25% of the dead load applied in the upward and downward directions. Thus, the design of a composite slab as a diaphragm to carry the vertical earthquake load will be very similar to that in gravity loads.

A composite slab must be designed to carry the factored design loads at the ultimate limit state. Longitudinal shear failure in the shear span L_s due to shear at the steel decking-concrete slab interface is the most common type of failure for medium-span slabs at the ultimate limit state. In Eurocode 4, the longitudinal shear capacity is assessed by using full scale laboratory tests of simply-supported slabs to measure slab performance. Full scale slab specimens are required because the longitudinal shear capacity is dependent on the geometry and flexibility of the particular type of steel decking, the size, location and spacing of the embossment on the decking, as well as on the slenderness of the slab (i.e. the span-to-depth ratio).

Current codes do not present a procedure to evaluate the longitudinal shear strength of continuous composite slabs and this is often assessed by full scale tests. In this paper, the results of three full-scale tests on continuous composite concrete slabs cast with using profile decking (KF70) that is widely used in Australia are presented. The slab specimens were tested in four-point bending at each span with shear spans of span/4. The longitudinal shear failure of each slab is evaluated and the measured mid-span deflection, the end slip and the mid-span steel and concrete strains are also presented and discussed. In addition, the slabs are modelled in finite element software using an interface element to model the contact between the slab decking and concrete slab.

EXPERIMENTAL STUDY

Three identical composite slabs were cast with trapezoidal decking profile KF70 supplied by Fielders Australia (2008) as permanent formwork and the concrete was then cured for 7 days under wet hessian. The shape and dimensions of the profile are shown in Fig. 1. The thickness of the steel decking was $t_{sd} = 0.75$ mm. The steel decking was completely supported on the laboratory floor during casting of the concrete to minimise any initial stress or deformation in the steel decking. Each slab was 6900 mm long, with a cross-section 150 mm deep and 1200 mm wide, and contained no bottom reinforcement (other than the external steel decking). Each specimen was continuous over the interior support and simply-supported on a roller at each of the two exterior supports. The centre-to-centre distance between the each exterior roller support and interior hinge support was 3350 mm. Longitudinal and transverse reinforcement was provided in the top of the slabs in the negative moment region over the interior support, as shown in Fig. 2b.



$A_{sd} = 1100 \text{ mm}^2/\text{m}$; $y_{sd} = 27.7 \text{ mm}$; $I_{z, sd} = 584000 \text{ mm}^4/\text{m}$
Figure 1. Dimensions (in mm) of steel decking profile KF70 ($t_{sd} = 0.75$ mm)

Each slab was tested with shear span of $L_s = L/4$ ($3350/4 = 840$ mm). Two load cells were placed underneath each support to measure the support reaction and its variation at any time. The deflection at the mid-spans and the end slip at both exterior supports were measured by using LVDTs. The strains in concrete and steel decking were measured at selected sections on the top and bottom surfaces of slabs using 60 mm long strain gauges. The strain in the longitudinal reinforcement at the interior support was measured by using embedded strain gauges. A schematic view of the experimental setup and the measured parameters are shown in Fig. 2a. The load was applied in a displacement control manner at a rate of 0.3 mm/min.

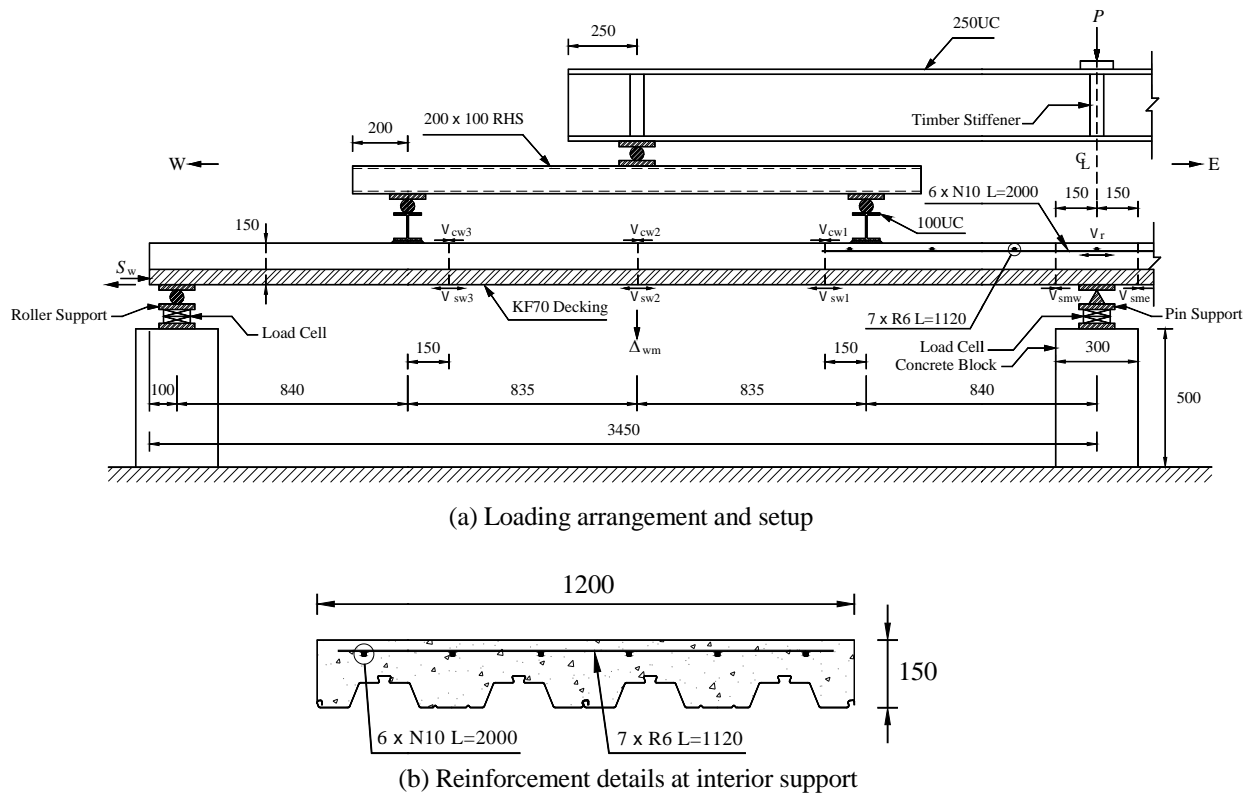


Figure 2. Test setup, measured parameters and cross-section at interior support

MATERIAL PROPERTIES

The mean compressive strength f_c and modulus of elasticity E_c of the concrete at the age of testing were determined from six standard 100 mm diameter cylinder tests and were 47.9 MPa and 33,050 MPa, respectively. The concrete flexural tensile strength $f_{ct,f}$ (modulus of rupture) was measured on 100 mm \times 100 mm \times 500 mm concrete prisms and was 4.68 MPa. The yield stress f_{yp} and the elastic modulus E_s of the steel decking were also measured on three coupons cut from the decking, and were 532 MPa and 203 GPa, respectively. Similarly, from three test samples of the reinforcing bars, the average values were $f_y = 495$ MPa and $E_s = 205$ GPa, respectively.

DISCUSSION OF TEST RESULTS

The mid-span deflection versus applied load for each slab is shown in Fig. 3a. First slip occurred after a significant proportion of the ultimate load had been applied and it resulted in a sudden drop in the applied load. Eventually, all slabs failed due to a loss of bond at the interface of the steel decking and the concrete slab. Even in the post-peak region after large deformations occurred, there was little vertical separation between the steel decking and concrete slab. At loads well below the load at which interface slip occurred in each slab, flexural cracks formed in the top surface at the interior support and between the applied loads and propagated into the cross-section. Cracking was associated with significant local increases in the tensile stress in the steel reinforcement at the interior support and tensile stress in the steel decking and compressive stress in the concrete in the top fibres between applied loads, as well as significant increases in slab deflection. Abrupt increases in mid-span deflection and end slip were observed after the loss of composite action.

Without exception, the widest crack occurred at the interior support and in the vicinity of one of the applied loads. After the peak load had been reached, wide cracks at the top surface of the interior support and below the applied line loads eventually divided the concrete. This was typically associated with excessive end slip. Significant post-slip strength was observed in all three slabs. The longitudinal shear failure mode is relevant to post-slip strength and behaviour of composite slabs. According to the Eurocode 4 definition of ductility, the longitudinal shear behaviour is considered to be ductile if the failure load exceeds the load

causing a recorded end slip of 0.1 mm by more than 10% and hence, all slabs failed in a ductile manner. Graphs of end slip versus applied load are shown in Fig. 3b.

The measured load causing an end slip of 0.1 mm $P_{(0.1\text{mm})}$, the peak load capacity P_{max} and the applied load at the end of the test P_{end} for each slab are summarised in Table 1. Also given in Table 1 are the deflection at peak load, the deflection at the end of the test, the maximum end slip (at the end of the test), the strain in steel decking at mid-span at the peak load and the strain in concrete at mid-span at the peak load. The mid-span deflections in the slabs at the peak load were highly variable, and ranged from span/176 for the western span to span/71 for the eastern span of slab S2, respectively.

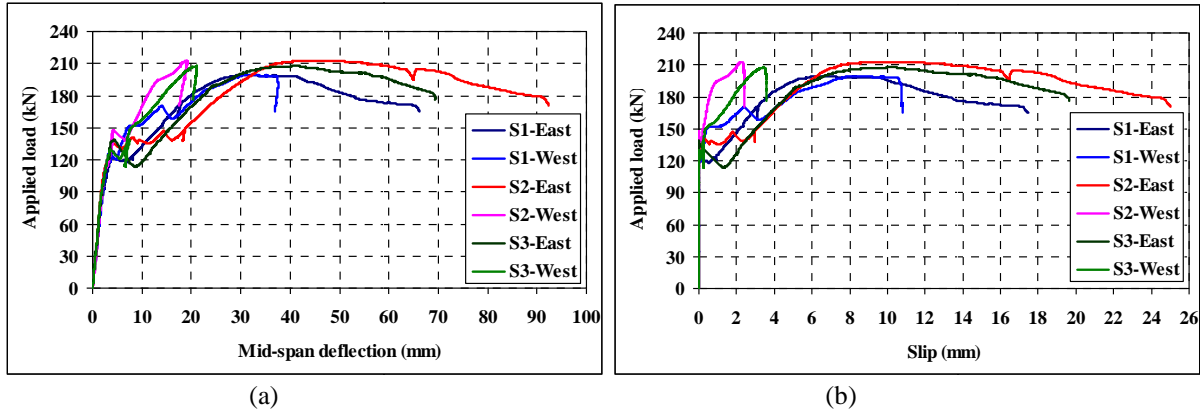


Figure 3. Mid-span deflection (a) and end slip (b) versus applied load

Table 1. Summary of test results

Slab	$P_{(0.1\text{mm})}$ (kN)	P_{max} (kN)	P_{end} (kN)	s_{max} (mm)	s_{end} (mm)	S_{max} (mm)	$s_{\text{m(max)}}$ (μ)	$c_{\text{m(max)}}$ (μ)
S1	120.5	199.8	165.0	E(30.9)	E(66.3)	E(17.5)	E(478)	E(197)
				W(31.8)	W(36.9)	W(10.8)	W(440)	W(138)
S2	133.8	213.0	170.5	E(46.8)	E(92.4)	E(25.0)	E(1290)	E(201)
				W(19.0)	W(17.6)	W(2.4)	W(1240)	W(202)
S3	123.1	208.4	176.6	E(40.4)	E(69.4)	E(19.6)	E(1041)	E(218)
				W(21.0)	W(20.3)	W(3.6)	W(787)	W(233)

s_{max} : deflection at peak load; s_{end} : deflection at the end of the test; S_{max} : maximum end slip (at the end of the test); $s_{\text{m(max)}}$: strain in steel at mid-span at peak load; $c_{\text{m(max)}}$: strain in concrete at mid-span at peak load.

The maximum value of the strain in the steel decking at mid-span at the peak load was measured at the eastern span of slab S2 and was $s_{\text{m(max)}} = 1290 \mu$. The steel yield strain is $s_{\text{yp}} = f_{\text{yp}}/E_s = 2620 \mu$ and therefore the maximum steel strains reached only 49% of the yield strain. Clearly, the loss of longitudinal shear stress in all slabs prevented the steel decking from yielding and the full plastic flexural capacity could not be reached. Fig. 4 shows slab S1 after reaching its peak load and just before termination of the test, and shows the different deflections in either span.



Figure 4. Final deflected shape of slab S1

FINITE ELEMENT ANALYSIS

General Structural Modelling

The general purpose finite element software ATENA 3D version 4.2.7 was used in the present study to investigate the ultimate strength of the continuous composite concrete slabs tested in the laboratory. ATENA 3D program is specifically designed for 3D non-linear finite element analysis of solids with rigorous constitutive relationships to model the behaviour of reinforced concrete structures including concrete cracking, concrete crushing and reinforcement yielding.

A three-dimensional (3D) finite element model was developed to account for the material and geometric nonlinearities in the composite slabs. The material properties selected for steel decking, concrete slabs and reinforcing bars were similar to the values obtained from tests on companion specimens as previously summarised.

The Newton-Raphson iterative solution method was chosen. The mid-span deflection of each slab versus the total load was monitored in the analysis. Four monitoring points at the location of the applied line loads and two monitoring points at mid-span were defined to monitor the amount of total load and mid-span deflection, respectively. All of the monitoring points were defined on the top surface of each slab.

Steel plates having 50 mm thickness and 100 mm width were modelled at the load application points to simulate the laboratory experiments and to prevent high stress concentrations at these locations. The partial connection allowing slip to occur between the steel decking and concrete slab was considered. Similar to the experimental study, in each analysis the load was applied in a displacement control manner.

The concrete slab, steel plates and steel decking were modelled with three dimensional solid linear tetrahedral elements with three translation degrees of freedom per node. Linear tetrahedral elements contain 4 nodes compared to the 10 nodes in quadratic elements, and hence require less computational effort and time to run the analysis. The global element size was limited to 50 mm.

In this study the reinforcement bars over the interior support were modelled as discrete bars with perfect bond to concrete. The reinforcing bars were modelled using “CC Reinforcement” material type with elastic-fully plastic behaviour without strain hardening.

Material Modelling

The steel plates at the load application points were modelled as a linear-elastic material using the “3D Elastic Isotropic” material type with $E_s = 200$ GPa. The steel decking and reinforcement were modelled as an elastic-fully plastic material without strain hardening using the “3D Bilinear Steel Von Mises” and “CC Reinforcement” material types, respectively. A bilinear stress-strain relationship was used for steel decking and reinforcement in both tension and compression. The Von Mises yield criterion was used in the non-linear analysis to treat the plasticity of steel material.

The concrete slab was modelled using the “3D Nonlinear Cementitious 2” material, for which its properties in different conditions were considered.

The behaviour of concrete in tension before cracking was assumed to be linear-elastic, i.e. $\dagger = E_c \nu$, where \dagger is the tensile stress in the concrete, E_c is the initial elastic modulus of the concrete and ν is the strain in the concrete. To model the tension in concrete after cracking, a fictitious model based on a crack-opening law and fracture energy (as shown in Fig. 5) was used in combination with the crack band theory for modelling concrete tension after cracking using:

$$\frac{\dagger}{f_t} = \left\{ 1 + \left(c_1 \frac{w}{w_c} \right)^3 \right\} \exp \left(-c_2 \frac{w}{w_c} \right) - \frac{w}{w_c} (1 + c_1^3) \exp(-c_2) \quad (1)$$

where w is the crack opening, w_c is the crack opening at the complete release of stress, $c_1 = 3$, $c_2 = 6.93$, $w_c = 5.14G_f / f_t$ and G_f is the fracture energy needed to create a unit area of stress-free crack and was taken as 30 N/m in the numerical model.

The stress-strain curve for concrete in compression is given in Fig. 6. The following equation recommended by the CEB-FIP Model Code (1993) was adopted for the ascending branch of the concrete stress-strain law in compression:



$$\dagger = f_c \left[\frac{kx - x^2}{1 + (k-2)x} \right], \quad x = \frac{v}{v_c}, \quad k = \frac{E_c}{E_{c1}} \quad (2)$$

where \dagger is the concrete compressive stress, x is a normalised strain, v_c is the strain at peak stress, E_c is the initial elastic modulus and E_{c1} is the secant elastic modulus at the peak stress. The shape parameter k may have any positive value greater than or equal to 1 (e.g. $k = 1$ linear, $k = 2$ parabolic).

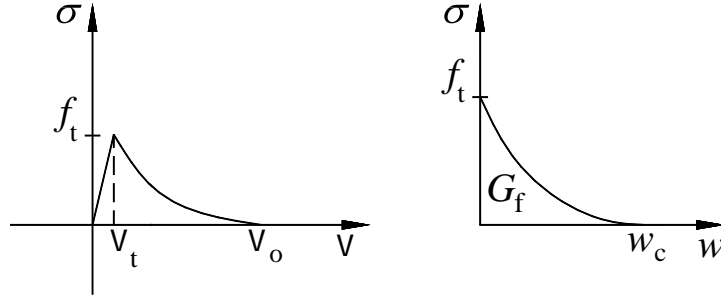


Figure 5. Stress-strain curve for concrete in tension

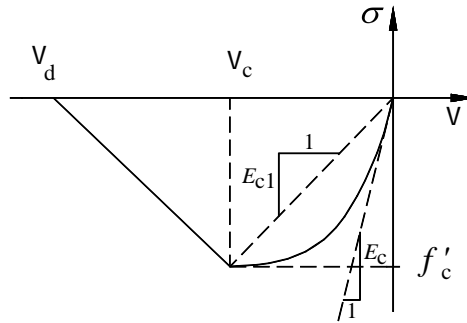


Figure 6. Stress-strain curve for concrete in compression

The softening law in compression is linearly descending. In this study, a fictitious compression model based on dissipated energy was used. The model is based on the assumption that compression failure is localised in a plane normal to the direction of the compressive principal stress. All post-peak compressive displacements and energy dissipation are localised in this plane. It is assumed that this displacement is independent of the size of the member. This hypothesis is supported by experiments conducted by van Mier (1986). The strain is given by the following expression:

$$v_d = v_c + \frac{w_d}{L'_d} \quad (3)$$

where w_d is the plastic displacement at the end of the softening curve taken as 0.5 mm, v_d is the limiting compressive strain and L'_d is the band size.

Steel Deck-Concrete Slab Interface

The “3D Interface” material type in ATENA 3D was used to model contact between the steel decking and the concrete slab. The interface material is based on the Mohr-Coulomb criterion with a tension cut off. The constitutive relation for a general two-dimensional case is given in terms of tractions on the interface planes and the relative sliding and opening displacements as:

$$\begin{Bmatrix} \dagger \\ \dagger \end{Bmatrix} = \begin{bmatrix} K_t & 0 \\ 0 & K_n \end{bmatrix} \begin{Bmatrix} \Delta_v \\ \Delta_u \end{Bmatrix} \quad (4)$$

The initial failure surface corresponds to a Mohr-Coulomb condition with an ellipsoid in the tension regime. After the stresses violate this condition, this surface collapses to a residual surface which



corresponds to dry friction. The frictional properties of the interface material model in ATENA 3D are defined by the shear cohesion c and the friction coefficient $\{\}$. The maximum shear stress is limited by the linear relation $\ddagger = c - \{\ddagger$, where \ddagger is the interface compressive stress. In tension, the failure criterion is replaced by an ellipsoid which intersects the normal stress axis at the value of f_t with the vertical tangent and the shear axis is intersected at the value of c with the tangent equivalent to $\{\}$. For this:

$$\ddagger = 0, \quad \ddagger > f_t \quad (5)$$

$$|\ddagger| \leq c - \{\ddagger, \quad \ddagger \leq 0 \quad (6)$$

$$\ddagger = \ddagger_0 \sqrt{1 - \frac{(\ddagger - \ddagger_c)^2}{(f_t - \ddagger_c)^2}}, \quad \ddagger_0 = \frac{c}{\sqrt{1 - \frac{\ddagger_c^2}{(f_t - \ddagger_c)^2}}}, \quad \ddagger_c = -\frac{\{\ f_t^2}{(c - 2\{\ f_t)} \quad 0 < \ddagger \leq f_t \quad (7)$$

The coefficients K_n and K_t in Eq. 4 represent the initial elastic normal and shear rigidities, respectively. There are two additional rigidity values that need to be specified in the ATENA 3D input (2009). They are denoted in Fig. 7 as $K_{n(\min)}$ and $K_{t(\min)}$. These values are used only for numerical purposes after the failure of the element, in order to preserve the positive definiteness of the global system of equations. Theoretically, after the interface failure the interface rigidity should be zero, which would mean that the global rigidity would become indefinite. These minimal rigidities are recommended to be about 0.001 times of the initial rigidities. The assumed values of $K_n = 1000 \text{ MN/m}^3$ and $K_t = 60 \text{ MN/m}^3$ showed the best agreement between the finite element model and the test results. Of course, these values are deemed to be a function of material properties and rigidities of the steel decking and the concrete slab. Vertical separation at the steel-concrete interface was assumed to be negligible, and was achieved by assigning a very large value for the initial elastic normal rigidity K_n in the model. The cohesion stress value of 0.1 MPa and tensile stress value of 0.5 MPa were selected for the interface element properties.

A summary of the comparison between the test results and the numerical results obtained from the partial interaction analyses is presented in Fig. 8. Good agreement was obtained between the experimental and numerical deflections.

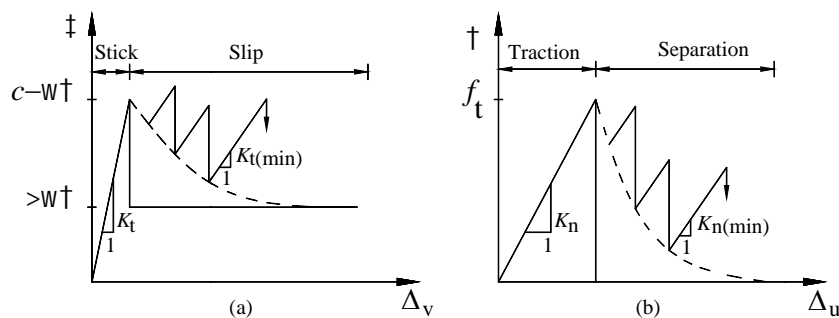


Figure 7. Interface model behaviour in (a) shear and (b) tension

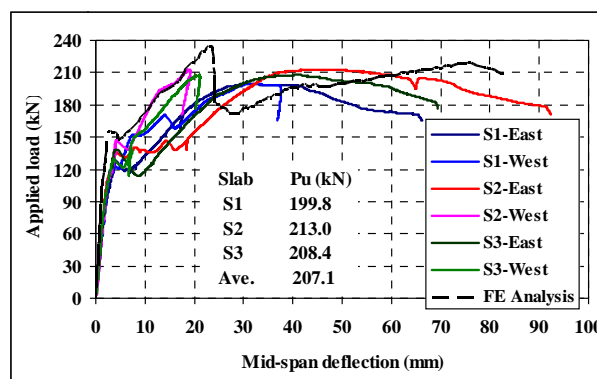


Figure 8. Load versus mid-span deflection comparisons.

CONCLUSIONS

The results of short-term testing to failure of three continuous composite slabs constructed using profiled steel decking section have been presented and discussed. The slabs were tested in symmetric four-point bending in each span. The slabs were then modelled in a finite element program and the results were compared with test results. Currently, national design standards do not present guidance for the design of continuous composite slabs, and full-scale testing is needed. In lieu of the expense involved with full-scale testing, the good agreement between the finite element modelling and the test results obtained in the study suggests that far less expensive numerical modelling can be used to verify the performance of continuous composite slabs.

REFERENCES

ATENA (2009) Program Documentation, Part 1: Theory Manual, Cervenka Consulting, Prague, Czech Republic

British Standards Institution (2005) EN 1994 Eurocode 4: Design of Composite Steel and Concrete Structures, Part 1.1 General Rules and Rules for Buildings, BSI, London, UK

CEB (1993) CEB-FIP Model Code 1990, London, Thomas Telford

Fielders Australia Pty. Ltd. (2008) Specifying Fielders KingFlor Composite Steel Formwork System, Design Manual

Reyes-Salazar A and Haldar A (2000) Consideration of Vertical Acceleration and Flexibility of Connections on Seismic Response of Steel Frames, *12th World Conference on Earthquake Engineering*, Auckland, New Zealand, Paper No. 1171

van Mier J.G.M. (1986) Multi-Axial Strain-Softening of Concrete. *Materials and Structures*, 19: 179-200

